

Conical second harmonic generation in one-dimension nonlinear photonic crystal

Ning An, Yuanlin Zheng, Huaijin Ren, Xuwei Deng, and Xianfeng Chen

Citation: *Appl. Phys. Lett.* **102**, 201112 (2013); doi: 10.1063/1.4807673

View online: <http://dx.doi.org/10.1063/1.4807673>

View Table of Contents: <http://apl.aip.org/resource/1/APPLAB/v102/i20>

Published by the AIP Publishing LLC.

Additional information on *Appl. Phys. Lett.*

Journal Homepage: <http://apl.aip.org/>

Journal Information: http://apl.aip.org/about/about_the_journal

Top downloads: http://apl.aip.org/features/most_downloaded

Information for Authors: <http://apl.aip.org/authors>

ADVERTISEMENT



**MATERIAL SCIENCE RESEARCH
AT 3K – MADE SIMPLE**

MONTANA INSTRUMENTS
COLD SCIENCE MADE SIMPLE

CLOSED CYCLE OPTICAL CRYOSTATS

Conical second harmonic generation in one-dimension nonlinear photonic crystal

Ning An,¹ Yuanlin Zheng,¹ Huaijin Ren,¹ Xuewei Deng,^{2,a)} and Xianfeng Chen^{1,b)}

¹Department of Physics, Key Laboratory for Laser Plasmas (Ministry of Education), Shanghai Jiao Tong University, 800 Dongchuan Road, Shanghai 200240, China

²Laser Fusion Research Center, China Academy of Engineering Physics, Mianyang, Sichuan 621900, China

(Received 21 March 2013; accepted 9 May 2013; published online 22 May 2013)

We observed conical second-harmonic generation in a one-dimension anomalous-dispersion-like medium, which manifests itself as scattering-assisted nonlinear interaction via quasi-phase-matching sum frequency process. The parameters for the ring-shaped second harmonic beam are analyzed experimentally and theoretically, which disclose the structure information of the nonlinear photonic crystal and imply potential applications as characterization methods. Furthermore, by varying the angles of incident beam, the conical beam can be significantly enhanced owing to collinear nonlinear coupling between the input beam and the scattering light.

© 2013 AIP Publishing LLC. [<http://dx.doi.org/10.1063/1.4807673>]

The process of efficient second-harmonic generation (SHG) is one of the most studied effects in nonlinear optics, which depends crucially on phase-matching relations between the two interacting lights. As in some degenerated sum-frequency generation (SFG) scenarios, one of the interacting beams could be substituted by the scattered one. This usually leads to many types of parametric scattering processes, which manifest themselves as particular light patterns—dots, lines, and rings. Since quasi-phase-matching (QPM) proposed by Bloembergen *et al.* in 1962,¹ it provides plenty of phase-matching geometries by diverse types of one- and two-dimensional $\chi^{(2)}$ nonlinear crystals. Lately, observation of scattering-assisted conical SHG in one-dimension (1D) quasi-periodical² and 2D periodical^{3,4} optical superlattice has been reported. Such processes involve the k vector of the input fundamental beam mixing with scattered ones to yield, in a QPM manner, a relatively enhanced second-harmonic wave. Meanwhile, the features of scattering signals reveal the structure information of the $\chi^{(2)}$ crystal and suggest potential applications on studying light scattering.

In addition, other essential types of noncollinear interactions in connection with SHG, such as nonlinear Bragg diffraction,^{5,6} nonlinear Cherenkov emission⁷ as well as nonlinear Raman-Nath diffraction,⁸ have been explored experimentally and theoretically.⁹ In the vast majority of previous studies, such parametric processes occur in 1D, 2D periodically poled ferroelectrics crystals, for example, LiNbO₃,¹⁰ LiTaO₃,¹¹ and KTiOPO₄,¹² which coincidentally are normally dispersive media. Recently, efforts have been made to theoretically explore the performance of the nonlinear Cherenkov radiation under anomalous dispersion,¹³ which shows substantially different features from that in normally dispersive medium and extends potential applications that are otherwise difficult to access. The experiment was later demonstrated in anomalous-dispersion-like media, where the authors simulated such an environment by utilizing crystal birefringence, fundamental, and harmonic beams with

different polarization.¹⁴ However, experiments referring to conical SHG in anomalous dispersion media are still missing.

In this letter, we report on the conical SHG in an anomalous-dispersion-like medium—1D periodically poled lithium niobate (PPLN) by illuminating the PPLN with pump propagating parallel to the domain wall. The phase-matching geometries and other characteristics of the parametric process are discussed. Furthermore, varying the incident angles of the fundamental wave (FW) leads to significant enhancement of second harmonic (SH) spots which are part of the ring-shaped SHG. Analysis on the salient features of the phenomenon indicates the enhanced SHG fulfills exact nonlinear Bragg diffraction condition.

In view of an elastic scattering QPM process, the phase-matching condition of SHG in 1D periodically poled $\chi^{(2)}$ crystal can be written as

$$\mathbf{k}_1 + \mathbf{k}'_1 + \mathbf{G}_m = \mathbf{k}_2, \quad (1)$$

where \mathbf{k}_1 , \mathbf{k}'_1 , and \mathbf{k}_2 are the wave vectors of the participating fundamental beam, scattering beam, and the SH beam, respectively. \mathbf{G}_m is the corresponding reciprocal vector and m is integer representing the order of reciprocal. \mathbf{k}'_1 , derived from \mathbf{k}_1 by scattering, is taken as consecutively and symmetrically spatial distribution (see Fig. 1(a)). Furthermore, there exists a constraint for the reciprocal vector $G_0^2 \geq k_2^2 - 2k_1k_2$ derived from Eq. (1) as illustrated in Fig. 1(b). In normally dispersive ferroelectric materials, the desired G is typically quite large and the corresponding cutoff period of the crystal is conceivable small, which is limited to submicron scale. For instance, the maximum threshold of the period is 1.13 μm with incidence at 1064 nm, beyond which no ring-shaped SH appears. However, fabrication of the periodically poled materials with sub- μm domain structures attaining an optically usable domain depth and large enough grating area remains a challenge.

On the contrary, Eq. (1) always holds for anomalous dispersion media. There is no minimum reciprocal vector limitation of anomalous dispersion material and the tunability of light sources is comparably wide, whereby makes it preferable

^{a)}Electronic mail: xwdeng@caep.ac.cn

^{b)}Electronic mail: xfchen@sjtu.edu.cn

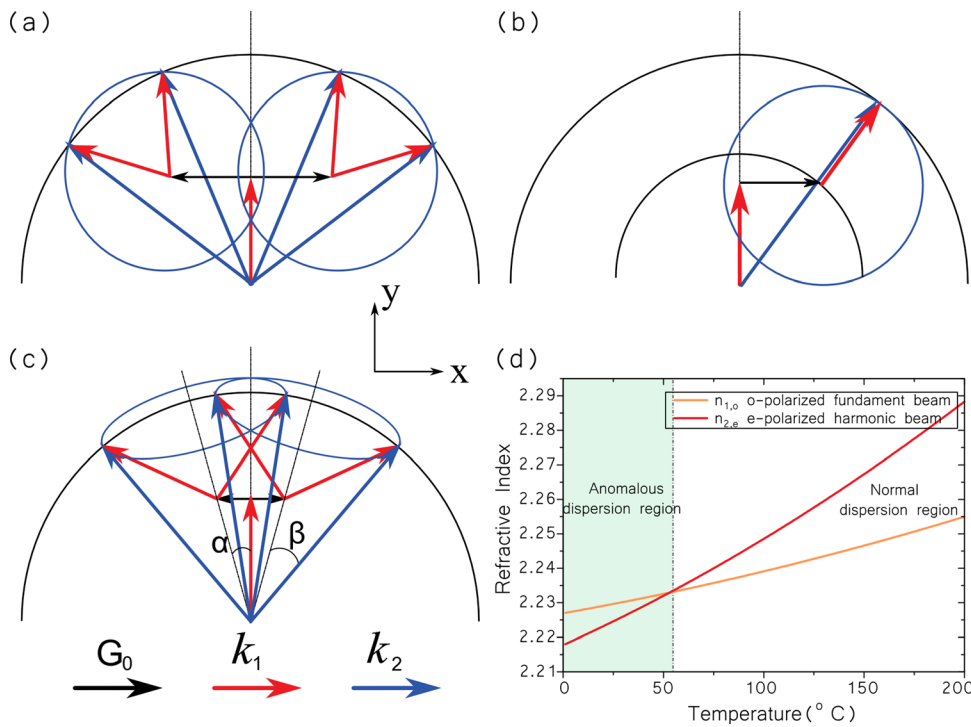


FIG. 1. Phase-matching geometries for (a) conical SHG under normal dispersion, (b) critical point of conical SHG with the semicircles corresponding to k_2 (outer) and $k_2 - k_1$ (inner), and (c) conical SHG while fundamental beam propagates along the domain wall under anomalous dispersion. (d) Theoretical curves of the refractive indices of ordinary-polarized fundamental beam and extraordinary-polarized second harmonic beam inside the sample.

scheme for studying light scattering (shown in Fig. 1(c)). Nevertheless, cases of SHG in an anomalous dispersion medium are conventionally difficult to acquire owing to both strong absorption near the optical resonance and difficult access of laser wavelength associated with such resonance of a nonlinear medium. Alternatively, by choosing a specific phase-matching scheme and utilizing the natural birefringence of the crystal, one can elaborately stimulate an anomalous-dispersion-like environment for SHG in normally dispersive medium to avoid such obstacle.¹⁴ In our experiments, it's noted that the refractive index curves of o-polarized fundamental exceeds e-polarized harmonic at the input wavelength of 1064 nm in 5 mol. % MgO: LiNbO₃ crystal at room temperature (see Fig. 1(d)). While taking into consideration the type I oo-e SHG phase-matching interaction scheme, it provides an ideal anomalous-dispersion-like medium here.

The domain structure of the sample using scanning electron microscopy (SEM) is illustrated in Figure 2(a), which exhibits nearly 1:1 duty ratio. The dimensions of the sample are 50 mm(x) \times 10 mm(y) \times 2 mm(z) with a poling period of $\Lambda = 30 \mu\text{m}$. A mode-locked Nd:YAG 1064 nm laser works as the fundamental wave source, which delivers 40 ps pulses with 0.4 mJ per pulse energy at a repetition rate of 10 Hz. The ordinary polarized laser beam is moderately focused (spots size $\approx 100 \mu\text{m}$) into the sample along y-axis.

In Figure 2(c) we display the projected image on the screen, which comprises several diffraction spots close to the pump spot and a set of symmetrically distributed ring-shaped SHG. The SH diffraction dots are the outcome of nonlinear Raman-Nath diffraction. The multiple conical SHG is corresponding to a reciprocal-dependent QPM process of incident beam and the scattered one. On the other hand, for normal incident beam, we didn't observe the nonlinear Cherenkov emission because the phase velocity of the nonlinear polarization does not exceed that of the harmonic beam under anomalous dispersion, which is consistent with our earlier work.¹⁴

Figure 1(c) schematically depicts the geometry of the phase-matching condition for the conical SHG emission in anomalous dispersion media. The multiple rings exhibit an axis-symmetrical distribution from $\vec{k}_{1,o}$, which are characterized by

$$\alpha = \arctan\left(\frac{|\vec{G}_m|}{|\vec{k}_{1,o}|}\right),$$

$$\beta = \arccos\left(\frac{|\vec{k}_{2,e}|^2 + |\vec{k}_{1,o} + \vec{G}_m|^2 - |\vec{k}_{1,o}|^2}{2|\vec{k}_{2,e}| \times |\vec{k}_{1,o} + \vec{G}_m|}\right), \quad (2)$$

where α is defined as the angle of symmetrical axis departed from $\vec{k}_{1,o}$, β defined as the half apex angle of conical beam $\vec{k}_{2,e}$. Furthermore, we explore the rule by recording these angles versus the periodicity of PPLN by using several samples with various poling periods (5.24 μm , 6.92 μm , 7.73 μm , 8.1 μm , 9.27 μm , 10.83 μm , 13.7 μm , 13.86 μm , 18.92 μm , 19.47 μm , and 30 μm), as illustrated in Fig. 2(d), which is consistent with the theoretical calculation.

The evolution of ring size and position projected on the screen varying with periods of samples is shown in Fig. 3. The pair of rings shrinks slightly in radius with the increase of periodicity of the samples. Meanwhile, the overlapping area of the symmetrical rings increases sharply. Therefore, the patterns of conical SH exhibit spatial distribution of the scattering signal, implying that measurements of ring centers and radii may be used for a nondestructive, noncontact detector to characterize the nonlinear photonic crystal.

Interesting phenomenon happens when one rotates the PPLN crystal around z-axis, whereby intensity peaks show up at the crossing points of conical SHG and nonlinear Raman-Nath diffraction in some specific angles (inset of Fig. 4(b)). To better understand the enhancement, one should consider the overall performance of SHG under anomalous

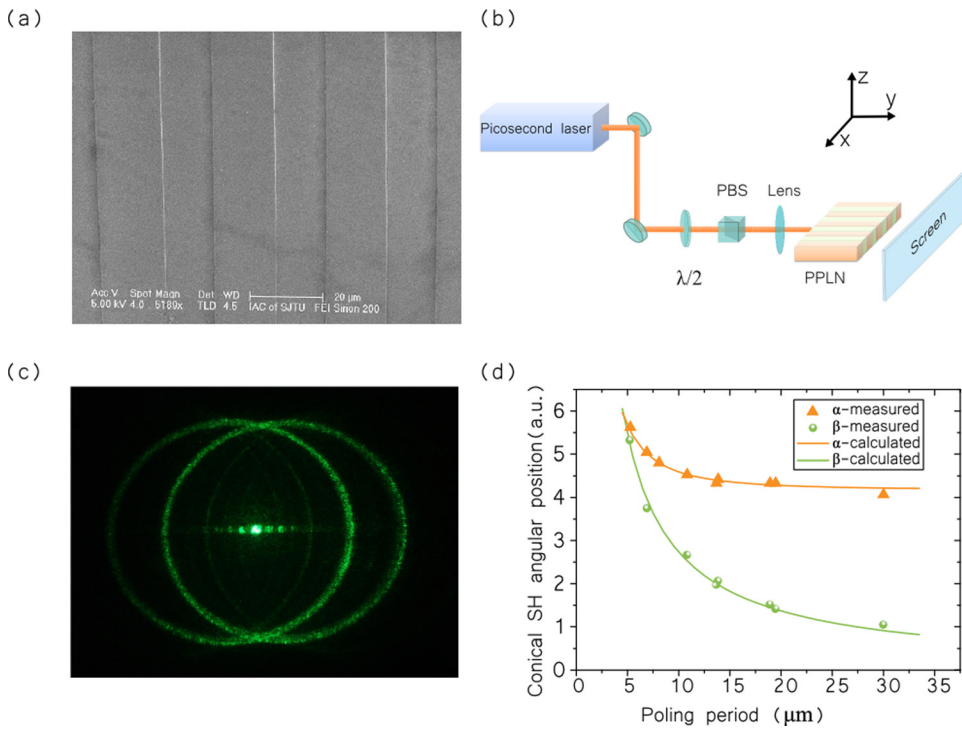


FIG. 2. (a) SEM image of the domain structure of the PPLN sample. (b) Layout of the experimental setup with fundamental beam propagating along the domain wall (y-axis). (c) Recorded patterns of the conical SHG and Raman-Nath diffraction. (d) Angle α and β as a function of the poling period Λ of the sample. Theoretical prediction (solid curves) and measured ones (signs) are in well agreement with each other.

dispersion. The azimuthal intensity distribution of the SH rings is described by

$$I_2 \propto I_1 I_1' d_{eff}^2 g_m^2, \quad (3)$$

where I_1 , I_1' , and I_2 are the intensities of the FW, the scattered FW, and their corresponding SHG, respectively, g_m is the Fourier coefficient of the reciprocal vector \mathbf{G}_m . As the scattering directions that correspond to the intensity maxima produced by paralleling to the input light satisfy to QPM condition, they can be interpreted by Eq. (3). For quasi-phase-matched noncollinear processes involving the incident beam and the low intensity scattered light, as the case in Fig. 2(c), the conical SHG intensity I_2 is comparably weak. While for some specific incident angles as the phase-matching geometry shown in Fig. 4(a), the interplaying of conical SHG and Raman-Nath diffraction yields, conceivably, a comparably strong I_2 . The schematic illustrates only the first-order reciprocal vector involved enhancement of the SHG emission. By altering the incidence

angles, one can achieve enhancement of the conical SHG multiple times corresponding to transversely phase-matching conditions at different orders of reciprocal vectors.

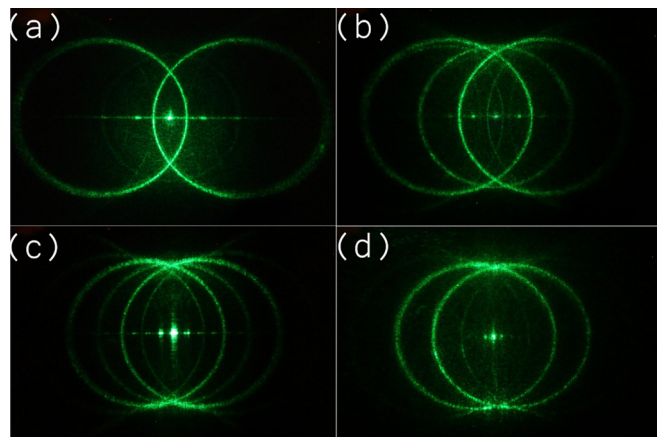


FIG. 3. Photos of multiple-conical SHG evolving with poling periods of the samples. (a-d) $\Lambda = 6.92 \mu\text{m}$, $10.83 \mu\text{m}$, $18.92 \mu\text{m}$, and $30 \mu\text{m}$, respectively.

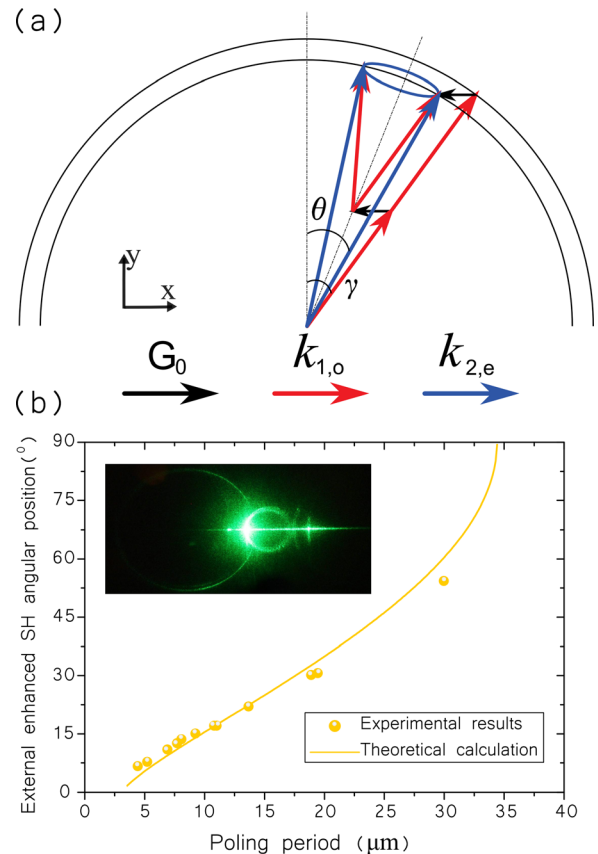


FIG. 4. (a) The phase-matching geometry for intensity peak position of the ring-shaped SHG. The semicircles are corresponding to $k_{2,e}$ (inner) and $2k_{1,o}$ (outer). (b) The first order reciprocal vector involved intensity maxima angles vary with periods of samples, solid curves for theoretical prediction, and signs for measured ones. The inset shows the projection of enhanced SH spot on the small ring-shaped SHG.

One can possibly find that the enhanced SH spot on the ring simultaneously fulfills both longitudinal and transverse phase-match conditions, which is actually nonlinear Bragg diffraction.^{15,16} The difference is that, in this case, it is anomalous nonlinear Bragg diffraction, which is described as

$$\begin{cases} 2k_1 \cos \gamma = k_2 \cos \theta, \\ 2k_1 \sin \gamma - k_2 \sin \theta = mG_0, \end{cases} \quad (4)$$

where γ is the incident angle of fundamental beam with respect to y-axis, θ is second harmonic angle. As has been verified in the experiment, the measured first order reciprocal vector involved intensity maxima angles of different periods of samples agree well with those determined from the nonlinear Bragg diffraction formula (Fig. 4(b)). Such remarkable enhancement reveals congruence of scattering conical SHG and nonlinear Bragg diffraction under anomalous dispersion, which broadens the access to efficient SHG for whole regions from anomalous dispersion to normal dispersion. The observed phenomena may also find potential applications in light scattering detecting, harmonic generation, as well as in control of the emission properties of SH signals.⁸

In conclusion, we proposed a scheme to obtain scattering-assisted SHG in 1D anomalous-dispersion-like medium which yields multiple conical SHG emission. With investigation on the conical SHG as a function of poling periods of the samples, one can learn the structure information of the crystal, which makes the conical SHG of great use in medium structure characterization. By varying the incident beam, the conical SH emission can be greatly enhanced owing to collinear nonlinear couplings between the input and scattering light, which shares the same phase-matching condition of nonlinear Bragg diffraction.

This work was supported in part by the National Basic Research Program “973” of China under Grant No. 2011CB808101, the National Natural Science Foundation of China under Grant Nos. 61078009, 61125503, 61235009, and 61205110, the Foundation for Development of Science and Technology of Shanghai under Grant No. 11XD1402600, and in part by the Innovative Foundation of Laser Fusion Research Center.

- ¹J. Armstrong, N. Bloembergen, J. Ducuing, and P. Pershan, *Phys. Rev.* **127**(6), 1918 (1962).
- ²Z. D. Xie, G. Zhao, P. Xu, Z. D. Gao, and S. N. Zhu, *J. Appl. Phys.* **101**(5), 056104 (2007).
- ³P. Xu, S. Ji, S. Zhu, X. Yu, J. Sun, H. Wang, J. He, Y. Zhu, and N. Ming, *Phys. Rev. Lett.* **93**(13), 133904 (2004).
- ⁴H. Huang, C. P. Huang, C. Zhang, D. Zhu, X. H. Hong, J. Lu, J. Jiang, Q. J. Wang, and Y. Y. Zhu, *Appl. Phys. Lett.* **100**(2), 022905 (2012).
- ⁵A. Shapira and A. Arie, *Opt. Lett.* **36**(10), 1933 (2011).
- ⁶S. M. Saltiel, D. N. Neshev, R. Fischer, W. Krolikowski, A. Arie, and Y. S. Kivshar, *Phys. Rev. Lett.* **100**(10), 103902 (2008).
- ⁷S. M. Saltiel, Y. Sheng, N. Voloch-Bloch, D. N. Neshev, W. Krolikowski, A. Arie, K. Koynov, and Y. S. Kivshar, *IEEE J. Quantum Electron.* **45**(11), 1465 (2009).
- ⁸S. M. Saltiel, D. N. Neshev, W. Krolikowski, A. Arie, O. Bang, and Y. S. Kivshar, *Opt. Lett.* **34**(6), 848 (2009).
- ⁹Y. Sheng, Q. Kong, W. Wang, K. Kalinowski, and W. Krolikowski, *J. Phys. B* **45**(5), 055401 (2012).
- ¹⁰N. An, H. Ren, Y. Zheng, X. Deng, and X. Chen, *Appl. Phys. Lett.* **100**(22), 221103 (2012).
- ¹¹H. X. Li, S. Y. Mu, P. Xu, M. L. Zhong, C. D. Chen, X. P. Hu, W. N. Cui, and S. N. Zhu, *Appl. Phys. Lett.* **100**(10), 101101 (2012).
- ¹²A. Fragemann, V. Pasiskevicius, and F. Laurell, *Appl. Phys. Lett.* **85**(3), 375 (2004).
- ¹³C. Luo, *Science* **299**(5605), 368 (2003).
- ¹⁴H. Ren, X. Deng, Y. Zheng, N. An, and X. Chen, *Phys. Rev. Lett.* **108**(22), 223901 (2012).
- ¹⁵I. Freund, *Phys. Rev. Lett.* **21**(19), 1404 (1968).
- ¹⁶K. Kalinowski, P. Roedig, Y. Sheng, M. Ayoub, J. Imbrock, C. Denz, and W. Krolikowski, *Opt. Lett.* **37**(11), 1832 (2012).